# Effect of vacancy defect clusters on the optical property of the aluminium filter used for the space solar telescope*

Cheng Xiu-Wei(程秀围)[a], Guan Qing-Feng(关庆丰)[a]†,
Fan Xian-Hong(范鲜红)[b], and Chen Bo(陈 波)[b]

[a] College of Material Science and Engineering, Jiangsu University, Zhenjiang 212013, China
[b] State Key Laboratory of Applied Optics, Changchun Institute of Optics, Fine Mechanics and Physics, Chinese Academy of Sciences, Changchun 130033, China

(Received 14 April 2009; revised manuscript received 11 May 2009)

We investigate the microstructures of the pure aluminium foil and filter used on the space solar telescope, irradiated by photons with different doses. The vacancy defect clusters induced by proton irradiation in both samples are characterized by transmission electron microscopy, and the density and the size distribution of vacancy defect clusters are determined. Their transmittances are measured before and after irradiating the samples by protons with energy $E = 100$ keV and dose $\phi = 6 \times 10^{11}/\text{mm}^2$. Our experimental results show that the density and the size of vacancy defect clusters increase with the increase of irradiation doses in the irradiated pure aluminium foils. As irradiation dose increases, vacancies incline to form larger defect clusters. In the irradiated filter, a large number of banded void defects are observed at the agglomerate boundary, which results in the degradation of the optical and mechanical performances of the filter after proton irradiation.

**Keywords:** proton irradiation, vacancy defect clusters, aluminium filter, optical performance

**PACC:** 6180, 6170E

## 1. Introduction

When thin metal films are subjected to irradiation with high energy particles, a high density of vacancy clusters is produced in the films.[1] Significant degradation in mechanical and physical performances can occur as a result of the formation of vacancy defect clusters.[2,3] This becomes a particular concern for thin metal films, because the degradation of material properties, owing to irradiation damage, will be the most problematic factor in determining the efficiency and lifetime of the irradiated materials.[4,5]

Aluminium film has been used for a long time as an optical filter on the Extreme-Ultraviolet Imaging Telescope (EIT) at the Solar and Hemispheric Observatory (SOHO) that is being used for imaging the solar corona,[6] and as mirrors on the Transition Region and Coronal Explorer (TRACE),[7] whose primary mission is to study magnetic fields and the associated plasma structures on the Sun. Both SOHO's EIT and TRACE instruments are still working after their service in space for 11 and 8 years, respectively.[7] However, space optics operate in a somewhat different environment from Earth optics. The main concern for space optics is their stability induced by the effect of space radiation bombardment, a likely environment for optics used in satellite instruments in the lower Earth orbit. Few studies are related to the space radiation effects on optical components. The discovery of Van Allen radiation belts in the early 1960s drew much attention from space craft designers.[8] Therefore, it is reasonably deduced that optical components exposed directly to space radiation, such as the filter, would be subjected to damage by charged particles in space radiation belts.

To understand the proton damage effect, it is necessary to investigate the microstructures of the irradiated samples. There are only a few reports in the literature about the microstructures in aluminium films irradiated by protons. The present work gives more detailed information about the microstructures in both irradiated pure aluminium foil and the optical filter.

*Project supported by the National Natural Science Foundation of China (Grant No. 50671042), the Program for Innovative Research Team of Jangsu University and the Program for Exellent Talents of Jangsu University (Grant No. 07JDG032).
†Corresponding author. E-mail: guanqf@ujs.edu.cn
© 2010 Chinese Physical Society and IOP Publishing Ltd

Additionally, the transmittances of the aluminium filter are also measured before and after being irradiated by protons with energy $E = 100$ keV and dose $\phi = 6 \times 10^{11}/\text{mm}^2$.

## 2. Experiment

Two types of pure aluminium films were selected as the target material. One kind of film was the annealed pure 99.9% polycrystalline aluminium foil used as a target in transmission electron microscopic (TEM) observation. These foils were prepared by mechanical prethinning, dimpling and, in the last step, electrolytic thinning of the thin plates until electron transparency occurred. The other one was an aluminium filter with about 1 $\mu$m thickness fabricated by the electron beam deposition method. After proton irradiation, both irradiated the aluminium foils and filter were directly applied to TEM observations. Microstructural examinations was conducted in an H-800 TEM operating at an acceleration voltage of 200 kV.

The irradiation experiment was conducted by using an irradiation simulator of space environment at room temperature. The proton irradiations were carried out under the following conditions: the proton energy is 100 keV, the vacuum in the test chamber is $4.2 \times 10^{-5}$ Pa, and current density is 0.1 $\mu$A/cm$^2$. Changes in transmittance of the optical filter before and after proton irradiation were examined by using a McPHERSON247 type of soft x-ray-extreme ultraviolet spectrometer.

## 3. Results and discussion

Typical microstructures of aluminium foils after proton irradiation are shown in Fig. 1. Proton irradiation at room temperature produced a higher number density of small defect clusters (generally below 20 nm) in all the irradiated samples. The defect clusters in aluminium foils look like almost black dots, and most of them were too small to allow determination of their morphology or crystallography from the images. Some larger defect clusters (arrowed region) were observed, indicating that the defect clusters consist predominantly of faulted loops on {111} planes (Frank loops). During a certain period of time after the start of electron irradiation in the TEM, these Frank loops became slightly shrunk, and some small defect clusters even disappeared. By this technique, based on Kiribati's analysis,[9,10] the majority of small point defect clusters observed after proton irradiation were identified as being of vacancy. In fact, molecular dynamics computer simulations of the dissociation of vacancy and interstitial Frank loops in copper and nickel demonstrated that the dissociation of Frank loops occurred more readily for vacancy than for interstitial loops.[11] It has also been found that the unfaulting of an interstitial loop requires a higher stress than that of a vacancy loop.[11] Based on the above arguments, the defect clusters observed are taken to be vacancy in nature, namely vacancy is the predominant means of diffusion in the aluminium foils.

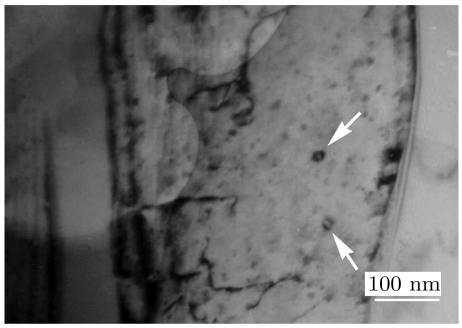



**Fig. 1.** TEM bright field image of Frank loops at $2 \times 10^{11}/\text{mm}^2$ dose.

The number density of defect clusters in each sample is plotted as a function of dose in Fig. 2. The cluster density in each sample increases with dose increasing from $1 \times 10^{11}$ to $4 \times 10^{11}/\text{mm}^2$, and reaches a peak value at $4 \times 10^{11}/\text{mm}^2$ dose. The cluster density of the sample at $6 \times 10^{11}/\text{mm}^2$ dose displays a small decrease compared with the sample at $4 \times 10^{11}/\text{mm}^2$ dose.

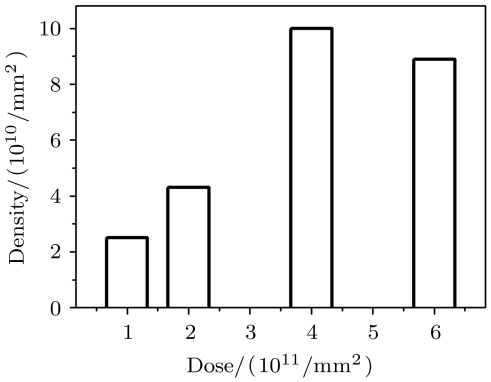



**Fig. 2.** Dependence of the number density of Frank loops on irradiation dose.

The size distributions of the small vacancy clusters are illustrated in Fig. 3. Frank loops clearly shift toward large sizes with increasing dose, suggesting that the vacancy Frank loops prefer to form larger clusters at high dose levels. The Frank loops have a mean size of up to more than 20 nm, and the size of the largest Frank loops reaches 50 nm at $4 \times 10^{11}/\text{mm}^2$ and $6 \times 10^{11}/\text{mm}^2$ doses respectively.

The TEM observation of the typical aluminium filter before proton irradiation is shown in Fig. 4. The pattern of the selected area electron diffraction, as shown in the inset in Fig. 4(a), indicates a random crystallographic orientation and fine aluminium grain structure. TEM dark field image shown in Fig. 4(b) reveals a fairly uniform grain and roughly equiaxed grains with an average grain size of about 10 nm and the largest grain size reaches about 20 nm. The grain interiors seem to be clean and no detectable defect structure was observed. Additionally, the microstructure of agglomerates consisting of several aluminium grains is formed as shown in Fig. 4(a). The average size (diameter) of the aluminium agglomerates was estimated to be about 80 nm from the range of images obtained (Fig. 4).

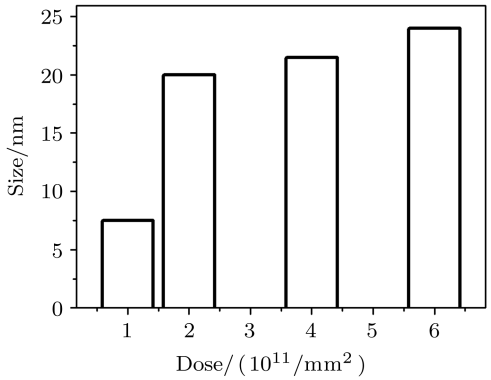



**Fig. 3.** Dependence of the size of Frank loop on irradiation dose.

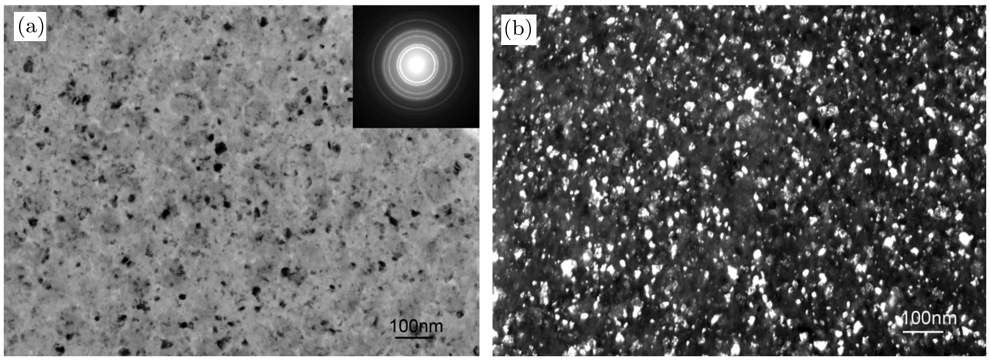



**Fig. 4.** TEM images of Al filter before irradiation, where panel (a) shows a bright field TEM image, and panel (b) displays a dark field TEM image.

The TEM images shown in Figs. 5(a) and 5(b) represent the typical microstructure of the irradiated filter at proton energy 100 keV, dose $6 \times 10^{11}$/mm$^2$ and $8 \times 10^{11}$/mm$^2$, respectively. The grain interiors are still clean and no detectable defect structure is observed. However, it is found that annular bands with brighter contrast could be visualised clearly as an agglomerate boundary. In an original filter sample (Fig. 4(a)), the contrast of initial agglomerate boundaries is very weak and it is not easy to determine their features. After proton irradiation, they become very clear. It is suggested that proton irradiation leads to the formation of agglomerate boundaries with brighter contrast.

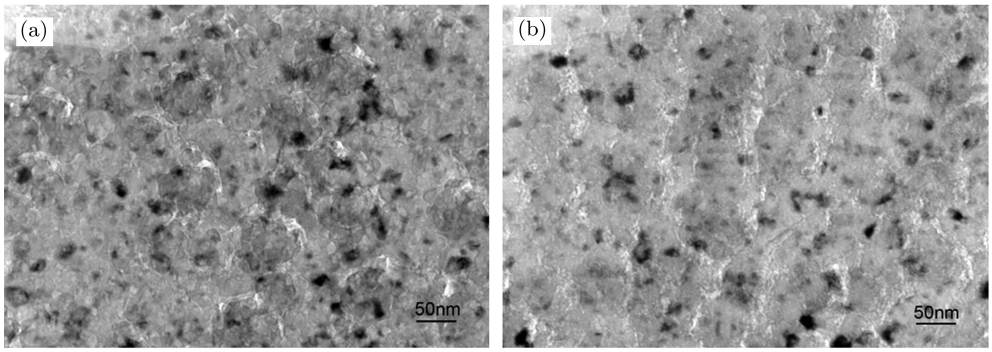



**Fig. 5.** TEM images of Al filter after irradiation by protons with dose (a) $\phi = 6{\times}10^{11}$/mm$^2$ and (b) $\phi = 8 \times 10^{11}$/mm$^2$.

Because there exists no fluid in a solid, the migration of atoms in a crystal can be achieved only by means of jumping step by step between adjacent lattice sites. In general, the lattice sites in a perfect crystal are occupied completely by natural atoms. Thus the migration of atoms is very difficult. However, after proton irradiation the presence of supersaturation vacancies in aluminium films provides a possibility for atom diffusion which results in the accumulation of vacancies and the formation of small point defect clusters just like the vacancy type Frank loops shown in Fig. 1. The experimental results of aluminium films suggest that these vacancies diffuse more readily to accumulate and form defect clusters with larger sizes at high dose levels.

There are two different ways of interaction when a proton beam irradiates materials, i.e. elastic scattering and inelastic scattering. A perfect crystal of grain interior with a periodic structure obeys Bragg's law which means that constructive interference (elastic scattering) occurs for a given wavelength and angle of incidence. In this case the protons of elastic scattering would go through the aluminium filter directly and have no energy loss, whereas the zones of grain and agglomerate boundary contain disordered atoms, just like amorphous structure. Most proton–filter interactions belong to the inelastic scattering type. The energy loss of the protons mainly changes into heat, causing the increase of temperature in these zones. Furthermore, the zones of agglomerate boundary have higher temperature values compared with the zones of grain boundary due to the bigger areas. As long as heat is redistributed under the influence of temperature, the zones of grain and agglomerate boundary are heated more rapidly, because the temperature of these zones increases at higher rates than the rates of its decrease in an interior part of the filter. As a result, most of the non-equilibrium vacancies migrate towards the zones of agglomerate boundary. The earliest vacancy migration paths are grain boundaries. This seems to result in the accumulation of vacancies near the zones of agglomerate boundary. Therefore, the local density of material seems to decrease near such defects, forming annular bands with brighter contrast in the regions of initial agglomerate boundaries. Figure 5 reveals that the widths of the bright bands formed become large with increasing dose. The widths of the bright bands, which can be estimated directly from Figs. 5(a) and 5(b), are ∼8 nm at $6 \times 10^{11}/\mathrm{mm}^2$ dose and ∼10 nm at $8 \times 10^{11}/\mathrm{mm}^2$ dose. Some bright bands are completely transparent and even become zonal or annular voids.

The production of vacancies and the formation of vacancy defect clusters in materials result in the macroscopic expansion and deteriorating toughness of materials, respectively. In fact, the ductility of the filter reduces evidently due to proton irradiation. During the course of TEM sample preparation, the irradiated filters were very breakable and not easy to manipulate. The samples irradiated with $8 \times 10^{11}/\mathrm{mm}^2$ dose were even broken into tiny fragments directly.

Proton irradiation results in degradation not only in toughness but also in the optical property of the filter. Figure 6 shows the transmittance spectra of the filter before and after proton irradiation at $6 \times 10^{11}/\mathrm{mm}^2$ dose as a function of wavelength in a range from 14 to 21 nm. We failed to prepare a usable sample irradiated at $8 \times 10^{11}/\mathrm{mm}^2$ dose for transmittance test due to fragmentation of the filter. Before proton irradiation, the profile of the transmittance spectrum is regular and only one peak is present at 17 nm wavelength. After proton irradiation, the transmittance increases obviously, the peak value increases from 12.1% to 15.0%, and the profile of transmittance spectrum becomes very irregular. Besides the peak at 17 nm wavelength, two sub-peaks at wavelengths of 19 nm and 20 nm are obtained, respectively. The results indicate that the transmittance performance of the aluminium filter is degraded by proton irradiation.

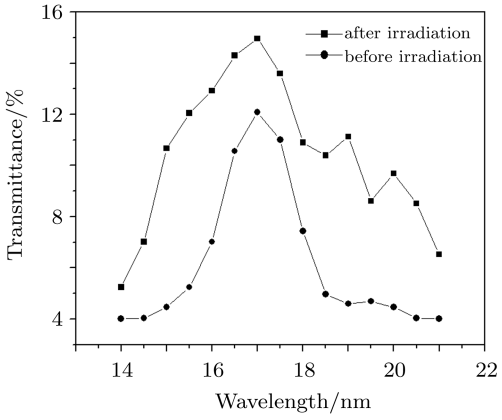



**Fig. 6.** Transmittances of Al filter before and after irradiation by protons.

## 4. Conclusions

In this work the change in optical constant caused by 100 keV proton irradiation for an aluminium filter is described. The transmittance spectrum of the filter

shows that degradation in the optical property of the filter can be induced by proton irradiation. In order to understand the proton damage effect, the microstructures of pure aluminium films and the optical filter after irradiation are investigated. The results show that a large number of vacancy defect clusters are introduced after irradiation and the density and the size of such defects increase with the increase of irradiated doses in the irradiated pure aluminium foils. As irradiated doses increase, vacancies are inclined to form larger defect clusters. For the irradiated aluminium filter, a large number of void defects with zonal or annular shape are formed at the initial agglomerate boundaries, which results in degradation of the optical and mechanical performances of the filter after proton irradiation.

## References


[1] Kiritani M 1999 *Rad. Eff. and Defects in Solids* **148** 233

[2] Dai Y, Bauer G S, Carsughi F, Ulmaier Lmaier H, Maloy S A and Sommer W F 1999 *J. Nucl. Mater.* **265** 115

[3] Juan J L, Jose A M and Jose A A 1996 *Opt. Commun.* **124** 208

[4] Dai Y, Jia X, Chen J C, Sommer W F, Victoria M and Bauer G S 2001 *J. Nucl. Mater.* **296** 174

[5] Liu H, Wei Q, He S Y and Zhao D 2006 *Chin. Phys.* **15** 1086

[6] Walker A B C, Barbee J T W, Hoover R B and Lindblom J F 1988 *Science* **241** 1781

[7] Bajt S, Edwardsb N V and Madeyc T E 2008 *Surf. Sci. Rep.* **63** 73

[8] Dauphin J and Radiat 1993 *Phys. Chem.* **43** 47

[9] Kiritani M, Yoshiie T, Kojima S, Tyoshi E, Kizuka Y and Matsunami N 1994 *J. Nucl. Mater.* **192** 212

[10] Kiritani M and Takata H 1978 *J. Nucl. Mater.* **67** 277

[11] Robach J S, Robertson I M, Lee H J and Wirth B D 2006 *Acta Mater.* **54** 1679